JOURNAL OF MATERIALS SCIENCE 24 (1989) 3686–3690

Detection of physical flaws in alumina reinforced with SiC fibres by NMR imaging in the green state

S. KARUNANITHY
Atlantic Research Laboratory, National Research Council of Canada, Halifax, Nova Scotia, Canada B3H 3Z1

S. MOOIBROEK
Bruker Spectrospin (Canada) Ltd, Milton, Ontario, Canada L9T 1Y6

Nuclear magnetic resonance (NMR) imaging can be applied non-destructively to detect physical flaws in fibre-reinforced ceramics in the green state. This paper describes the application of NMR imaging to detect physical flaws such as fibre-agglomerates and pores in ceramic matrix composites made by slipcasting. Application of this technique to detect and eliminate the composites with these flaws in the green state will result in considerable savings in processing time and in the cost of components or prototypes fabricated by slipcasting.

1. Introduction

A ceramic matrix may be reinforced with fibres in order to improve such mechanical properties as fracture strength and toughness. In this respect, silicon carbide and carbon fibres are being actively explored as reinforcements for ceramic matrices such as alumina, silicon carbide and silicon nitride. When incorporated into a ceramic matrix these fibres have been observed to pull out during fracture, as required for toughening [1–3]. However, due to the presence of open pores at the fibre/matrix interface, crack propagation sometimes occurs with little resistance from the fibres.

Recent results [3] have shown that such interfacial pores could be filled by a coating material which is strong enough to transfer the load from the matrix to the fibres, but weak enough to allow the fibres to pull out during the fracture. However, elimination of such pores, which are in the range of 1 to 3 μm in size [3], is not sufficient for the fabrication of reliable components from these materials. There are several other factors such as agglomerates, metallic inclusions, and pores formed during the formation of the green compact, all of which can either cause fracture of the composite or contribute to the formation of even larger flaws [4, 5]. Certain types of fabrication defects, such as agglomerates of the powder, can be eliminated or reduced in severity by careful manipulation of the starting materials. However, the agglomeration of fibres during the fabrication of fibre-reinforced composites is more difficult to avoid [5]. Therefore, in many cases, the average property of the composite may be suitable for the intended application, but a significant fraction of the components made from that material will be unsuitable due to the presence of damaging flaws.

A considerable improvement in the reliability and cost efficiency of these materials can be achieved by a complete examination in the green state, where most of the conditions that contribute to the fracture originate [6]. However, non-destructive examination of the green body is restricted by its fragility, rendering such techniques as ultrasonic scanning, which require contact of the detectors on the surface of the material, rather inadequate due to the possibility of introducing additional flaws [4]. In this respect, techniques such as nuclear magnetic resonance (NMR) imaging, in which physical manipulation of the sample is minimal, are more suitable for non-destructive testing of green-state materials.

This paper presents the results of an investigation into the application of NMR imaging as a non-destructive, non-invasive technique to detect physical flaws in green state fibre-reinforced ceramic matrix composites. The application of NMR imaging in this field has so far been restricted to monolithic ceramics, in which the green bodies and partially sintered ceramics were impregnated with "filler" fluids to provide detectable NMR signals [7–10]. In this work, alumina–SiC fibre composites were fabricated by slipcasting, and NMR imaging was applied to identify physical flaws in the green state, using water already present in the material.

NMR imaging experiments were first reported in 1973 [11], and development of several different approaches to data acquisition and processing followed thereafter (see, for example, reviews [12–14]). We have employed the two-dimensional spin warp method [15], which has its origin in the two-dimensional Fourier Zeugmatography method suggested by Kumar *et al.* [16]. This technique uses a standard 90° pulse–delay–180° pulse–delay–echo sequence in which the 90° pulse, and occasionally the 180° pulse, are selective. A field gradient is applied along the direction of the magnetic field (z) during the selective pulse(s) in order

0022–2461/89 $03.00 + .12

to control the width of the cross-section, or slice, of the sample in which the NMR signal is excited. A second gradient, applied orthogonal to the z gradient immediately following the 90° pulse and during the acquisition of the echo signal, provides frequency encoding, while a third gradient, orthogonal to the first two, is incremented stepwise for phase encoding. These latter two gradients yield spatial information in the plane of the cross-sectional slice.

While this technique is commonly used in the biological sciences [17], this is the first report on the application of NMR imaging to fibre-reinforced ceramic matrix composites in the green state.

2. Experimental details

Two samples were fabricated by slipcasting slurries of alumina (Reynolds RC-HP-DBM) containing 20 vol % SiC fibres (Nicalon fibres, diameter 8 μm and length 1 mm, supplied by DOW Chemicals, USA). The fibres were washed with acetone to remove the organic sizing (polyvinyl acetate) present on them. Dried fibres were then added to an alumina slip to give a total solids content of 60 wt %. For casting sample 1, this slurry was mixed in an Heat Systems Ultrasonicator for 2 min and the pH was adjusted to 5.2 to obtain a well-flowing slip with viscosity of 25 mPa S. For sample 2, the pH of the above slip was adjusted by adding 0.005 N NH_4OH dropwise while stirring the slurry vigorously until it reached a partially flocculated state (pH 6.2). This flocculated slip was used for casting the composite.

Slipcasting was carried out using plaster moulds. Because the primary objective of this experiment was to investigate the applicability of NMR imaging to detect all possible physical flaws in the green composite, efforts were not made to remove trapped air in the slip by evacuation before pouring it into the mould. Slipcast samples of cylindrical shape (8 mm diameter and 20 mm high), were sealed in 10 mm o.d. NMR tubes as soon as their surface was dry enough to handle. A moist atmosphere was maintained over the samples to prevent further loss of water.

NMR imaging was carried out using a Bruker MSL 400 MHz spectrometer equipped with a micro-imaging accessory. The images shown in Figs 1 and 2 were obtained using a 10 mm Helmholtz coil included in the standard Bruker imaging accessory package. A "soft" 90° pulse of 1.8 msec duration and a "hard" 180° pulse of 54 μsec duration were employed in the imaging sequence. *TE*, defined as the time from the centre of the soft 90° pulse to mid-echo, was 8 msec, and *TR*, the delay between repetitions, was set to 500 msec. Sixteen scans were acquired at each of 256 phase-encoding steps, for a total acquisition time of approximately 34 min per image. Resolution of 70 × 70 μm^2 was achieved with X, Y gradients of 9.6 G cm^{-1} and acquisition of a 256 × 256 data point matrix. Slice thickness in each image is approximately 800 μm or 0.8 mm.

3. Results and discussion

3.1. General information

As in all NMR techniques, nuclei of a single isotope are observed selectively in NMR imaging, and generally ^1H is chosen due to its high receptivity. A typical

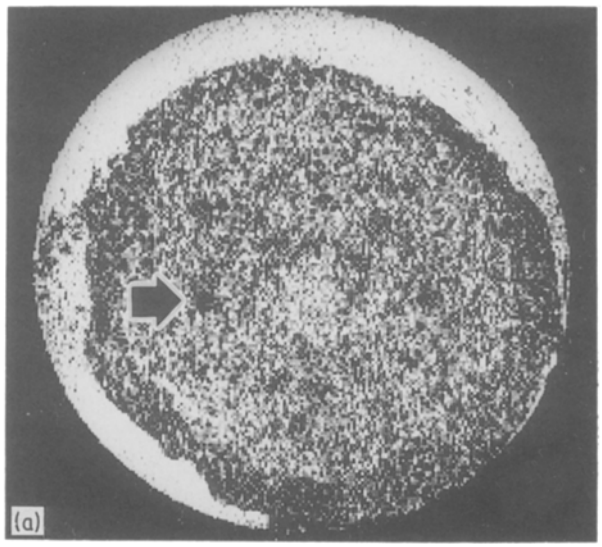

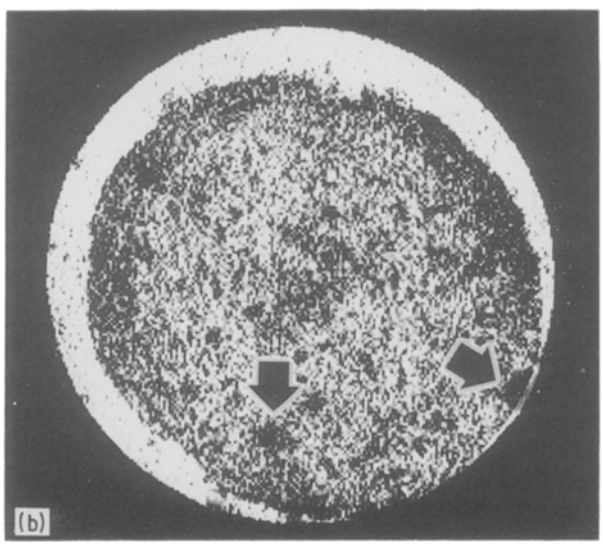

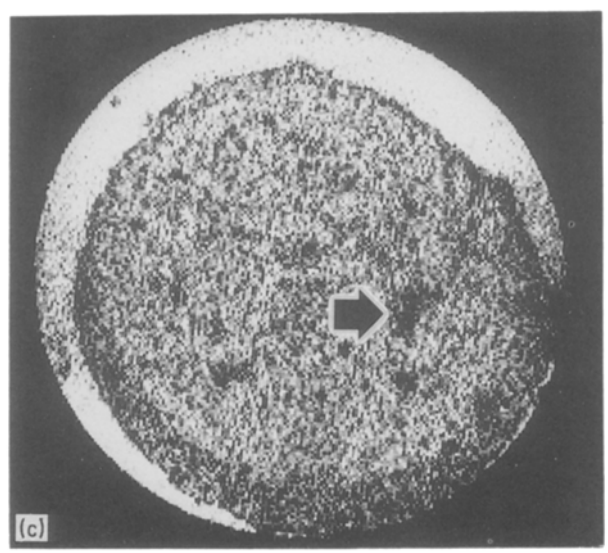

Figure 1 Proton NMR images of three 800 μm thick "slices" of sample 1, spaced 4 mm apart. The pixel resolution in each case is 70 × 70 μm^2. The diameters of the flaws marked with arrows are (a) 300 μm, (b) 350 μm (flaw near edge) and 375 μm (flaw near centre), (c) 425 μm. Diameter of the tube is 9 mm.

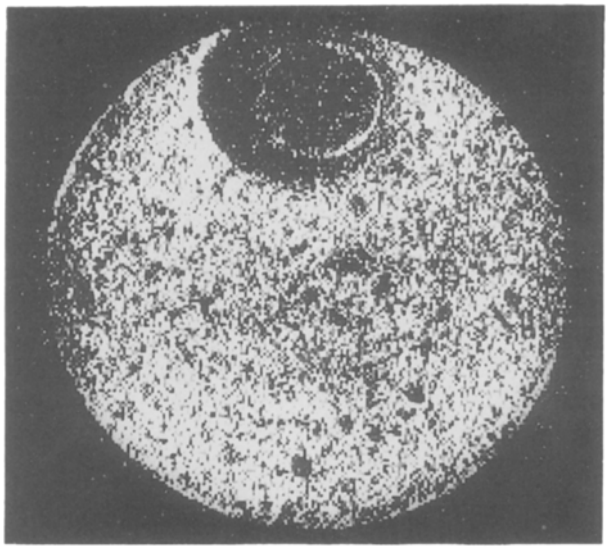

Figure 2 Proton NMR image of a slice centred 12 mm down from the top of sample 2, showing an area with an air bubble trapped within the green body. The quality of the image is affected by the magnetic susceptibility difference between water and air. Voxel resolution is $70 \times 70 \times 800\,\mu m^3$.

experiment is to image the distribution of water throughout a sample [12-14].

Representative images obtained from samples 1 and 2, fabricated according to the procedure described in Section 2, are shown in Figs 1 and 2. These images reflect the relative amount of ^1H spin density (i.e. the amount of water) across a transverse cross-section or "slice" through the sample. Bright areas in these images indicate high water content and dark areas represent pockets of air between particles or large physical flaws such as inclusions and agglomerates of fibres.

The spatial resolution of these images, $70 \times 70\,\mu m^2$ for an $800\,\mu m$ thick slice, is a considerable improvement over that reported earlier for ceramic samples [7–10]. Such high resolution is achieved by a combination of several critical factors, including the method of sample preparation, use of modern high-field NMR instrumentation, and optimization of pulses and delays in the imaging sequence.

3.2. Sample preparation

The earlier NMR imaging experiments on ceramics [7–10] depended upon impregnation of green bodies and pre-sintered samples with a "filler" liquid to provide detectable NMR signals. Particular disadvantages of this procedure are that the filler liquid may not permeate the entire sample and that flaws may be created by the separation of particles in the green body during vacuum impregnation. In addition, use of a relaxation agent in the filler fluid, such as chromium acetylacetonate, introduces metallic impurities which may be retained in the sample after the analysis.

These limitations are avoided in the method utilized here, in which the sample is fabricated by slipcasting from a water-based slurry. During the formation of the alumina slip, water molecules are adsorbed on to the surface of individual grains and retained throughout the casting process, during which the water acts as a binder. Water is therefore retained in the core of the sample, creating ideal conditions for NMR imaging. The slipcasting method has the further advantage that the amount of water retained in the sample can be controlled by the choice of drying conditions or partial flocculation of the slip.

3.3. Instrumentation

The NMR signal intensity is directly proportional to the number of protons in each resolvable volume element (voxel), therefore, any increase in resolution (with a concommitant decrease in the volume element) is accompanied by a decrease in sensitivity. However, the sensitivity of the NMR experiment also has a direct field (B_0) dependence, which increases as $B_0^{3/2}$ [18]. Performing imaging experiments on a high-field instrument, where $B_0 = 9.2$ Tesla (^1H frequency = 400 MHz), thus offers substantial gains in sensitivity, and consequently resolution, over more conventional lower field instruments.

For small samples, use of a high resolution NMR spectrometer and a micro-imaging accessory also has advantages in the high degree of homogeneity in applied field and rapid gradient switching times. Ramping gradients on and off quickly can create eddy currents within the magnet bore, which may destroy the field homogeneity and hence, the NMR signal. These eddy currents are minimal in the high resolution (89 mm bore) magnet/micro-imaging probe system, because the relatively small gradient coils, located close to the sample, require minimal power input to achieve high gradient strengths, and have little interaction with the probehead or magnet bore. With minimal delays necessary for gradient stabilization, several milliseconds can be trimmed from the time between the 90° pulse and acquisition of the echo signal (TE) in the imaging sequence. A short TE provides a real advantage in minimizing loss of signal due to diffusion or spin-spin relaxation. The importance of the latter factor is discussed briefly here; for a more general discussion reference [17] is suggested.

3.4. T_2, TE and resolution

Following the excitation of nuclear spins by an r.f. pulse, equilibrium is regained by two types of relaxation processes, governed by the rate constants T_1 and T_2. T_1 refers to an exchange of energy between nuclear spins and their surroundings (the "lattice"), and determines how rapidly the pulse-acquisition sequence can be repeated. The second relaxation constant, T_2, is associated with energy exchange between coupled spins rather than with the "lattice", and is related to the decay of observable magnetization and the resonance linewidth. Short T_2 values, found for spins in the solid state or solid-like environments, therefore, present experimental difficulties because of the very rapid decay of observable signal and the resultant broad lineshape. Rapid loss of observable signal demands a short TE time, which in turn limits digital resolution because TE incorporates the acquisition time.

The sample preparation technique used here produced a relatively narrow ^1H NMR water lineshape, with a T_2 of approximately 10 msec. To maintain as

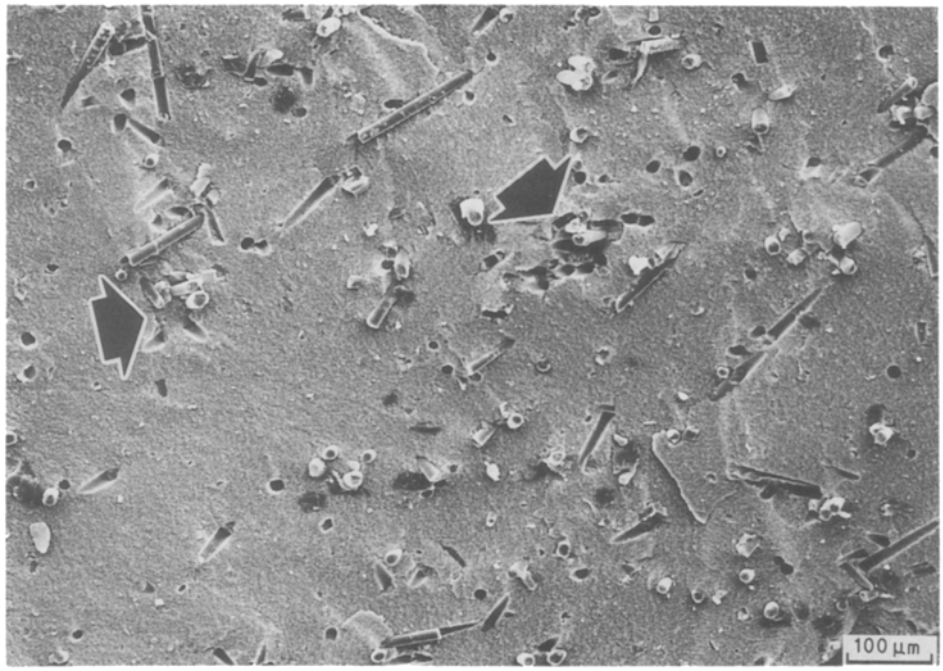

Figure 3 Scanning electron micrograph of a fracture surface of sample 1, after heat-treatment to the presintered state. Arrows indicate the areas of fibre agglomeration.

much digital resolution as possible, *TE* was minimized by substituting a hard 180° pulse for a longer soft pulse, and gradient stabilization delays were reduced to less than 0.5 msec, while keeping the data acquisition time relatively long (5.12 msec). The combination of sample preparation technique, high-field instrumentation and judicious choice of acquisition and echo times thus yielded the voxel resolution of $70 \times 70 \times 800\,\mu m^3$ shown in Figs 1 and 2.

3.5. Images of samples 1 and 2

Representative ^{1}H NMR images of sample 1 are shown in Fig. 1; an image of sample 2 is shown in Fig. 2. Sample 1 was fabricated with a fully deflocculated slip, and therefore would be expected to lose water faster than sample 2. Because magnetic susceptibility differences between water and air can detract from image quality, a small amount of water was added to the sample in order to remove air bubbles between the sample and the NMR tube. The additional water, apparent in the ^{1}H NMR images (Fig. 1) as a bright crescent around the ceramic, can be evaporated after imaging without harm to the composite.

The detrimental effect of air bubbles is demonstrated in Fig. 2. Although sample 2 was cast from a partially flocculated slip, which is known to deposit with higher and more uniform water content on the mould [19], water loss between the surface of the sample and the glass tube nonetheless created large pockets, adversely affecting the NMR images (Fig. 2).

Fibre-reinforced composites are very porous in the green state, due to the loose packing of the ceramic grains around the fibres [3]. The fine distribution of small bright spots across the ^{1}H NMR image (Figs 1 and 2) indicates the presence of water present in these open porosities; the dark spots or areas indicate flaws in the composites, caused either by foreign particles picked up in the powder processing step, or open pores and fibre bundles formed during the casting process. Dimensions of the larger flaws detected in the NMR images (Fig. 1), were measured using an image processor, and are noted along with the location of the image slice in the figure caption.

These flaws are much larger, and thus more easily detected in the green state than in pre-sintered material, as demonstrated by a scanning electron micrograph of a fracture surface of sample 1 (Fig. 3), obtained after heating the dried sample at 1100° C for 30 min in a vacuum furnace. The heat treatment adds strength to the composite, but causes essentially no overall size reduction. However, the porosities observed in the pre-sintered material (Fig. 3), are significantly smaller than those observed in the NMR images of the same composite in the green state (Fig. 1).

The differences in the observed porosity size is due not only to contraction of the alumina matrix around the SiC fibres during the heat treatment, but also due to the lack of water surrounding the fibre agglomerates, even in the green state. The fibre agglomerates, being composed of sintered SiC fibres, do not adsorb surface water, and therefore appear larger in ^{1}H NMR images, which detect the absence of water.

Because the strength of a composite is inversely dependent upon the size of the largest defect present [20], the extent to which the largest flaws detected in the green state are reduced by the sintering process is of interest. A detailed investigation into the change in size of the pores during the sintering process is being carried out in this laboratory.

4. Conclusion

This study shows that the samples slipcast from water-based slurries provide ideal conditions for ^{1}H NMR imaging. The occurrence of physical flaws such as fibre-agglomerates, foreign inclusions and open pores in the core or on the surface of the green-

state composite can be detected using this technique. Adaptation of this non-invasive and non-destructive technique to characterize the composite materials in the green state should result in higher reliability of the fabricated components.

Acknowledgements

The authors are grateful to Dr Colin Fyfe for the instrument time on the MSL 400 at the University of British Columbia, and also wish to thank Dr C. Rodger and Dr H. Stronks for their help in the preparation of this manuscript. This paper is issued as NRCC No. 30320.

References

1. W. B. HILLIG, *Ann. Rev. Mater. Sci.* **17** (1987) 341.
2. R. W. DAVIDGE, *Composites* **18** (1987) 92.
3. S. KARUNANITHY, *Mater. Sci. Engng* **A108** (1989) 221.
4. P. S. NICHOLSON, *Can. Ceram. Q.* **60** (1987) 26.
5. D. B. MARSHALL and J. E. RITTER, *Amer. Ceram. Bull.* **66** (1987) 309.
6. R. W. McCLUNG and D. R. JOHNSON, *MRS Bull.* **13** (1988) 34.
7. W. A. ELLINGSON, J. L. ACKERMAN, J. D. WEYAND, R. A. DIMILIA and L. GARRIDO, *Ceram. Engng Sci. Proc.* **8** (1987) 503.
8. J. G. ACKERMAN, L. GARRIDO, W. A. ELLINGSON and J. D. WEYAND, in "Non-destructive testing of high performance ceramics" (American Ceramic Society, Westerville, Ohio, 1987) p. 88.
9. J. G. ACKERMAN, *Polym. Prepr. (Am. Chem. Soc. Div. Polym. Chem.)* **29** (1988) 88.
10. L. GARRIDO, J. G. ACKERMAN, W. A. ELLINGSON and J. D. WEYAND, *ibid.* **29** (1988) 97.
11. P. C. LAUTERBUR, *Nature (London)* **242** (1973) 190.
12. P. A. BOTTOMLEY, *Rev. Sci. Instrum.* **53** (1982) 1319.
13. S. L. SMITH, *Anal. Chem.* **57** (1985) 595A.
14. M. A. FOSTER and J. M. S. HUTCHINSON, *J. Biomed. Engng* **7** (1985) 171.
15. W. A. EDELSTEIN, J. M. S. HUTCHINSON, G. JOHNSON and T. W. REDPATH, *Phys. Med. Biol.* **25** (1980) 751.
16. A. KUMAR, D. WELTI and R. R. ERNST, *J. Magn. Reson.* **18** (1975) 69.
17. D. D. STARK and W. G. BRADLEY (eds), "Magnetic Resonance Imaging" (Mosby, St Louis, 1988).
18. A. ABRAGAM, in "The Principles of Nuclear Magnetism" (Oxford University Press, London/New York, 1961).
19. J. E. FUNK, *Adv. Ceram.* **9** (1984) 76.
20. B. R. LAWN and T. R. WILSHAW, in "Fracture of Brittle Solids" (Cambridge University Press, London, 1975).

Received 31 October
and accepted 18 November 1988